Organic Process Research & Development **2010**, *14*, 1347–1357

Overcoming the Challenges of Solid Bridging and Constriction during Pd-Catalyzed C−N Bond Formation in Microreactors

Ryan L. Hartman,[†] John R. Naber,[‡] Nikolay Zaborenko,[†] Stephen L. Buchwald,*[,‡] and Klavs F. Jensen*[,†]

Department of Chemical Engineering, and Department of Chemistry, Massachusetts Institute of Technology, 77 Massachusetts Avenue, Cambridge, Massachusetts, U.S.A.

Abstract:

We investigate the mechanisms that govern plugging in microreactors during Pd-catalyzed amination reactions. Both bridging and constriction were shown to be important mechanisms that lead to clogging in our system and greatly limited the utility of microsystems for this class of reactions. On the basis of these observations, several approaches were engineered to overcome the challenge of plugging and to enable the continuous-flow synthesis of a biarylamine. Bridging could be eliminated with acoustic irradiation while constriction was managed via fluid velocity and the prediction of growth rates.

1. Introduction

The problem handling of solids in microfluidic systems has gained considerable attention in recent years as many interesting applications, from the manipulation of biological materials to a wide range of organic chemistry reactions, involve heterogeneous mixtures. For example, many important reactions in the synthesis of fine chemicals, including active pharmaceutical ingredients (APIs), require more than one phase, be it gas and liquid, liquid and liquid, or solid and liquid.[1−3] Microreactors have been widely applied in research to advance a deeper understanding of the physical and chemical rate processes that govern reactions,[4−16] yet their use for reactions involving solids has been relatively limited.[17−33] Understanding why solids lead to clogging in microsystems and the development of strategies to overcome this challenge are necessary to apply microsystems to a wider range of reaction discovery and process optimization.

A number of creative strategies have been employed to handle solids in both microreactors and simple microfluidic systems. While immobilization of the particles (e.g., catalyst or solid-supported reagent) can minimize the risk of microchannel clogging,[17−20,27] regenerating a packed bed necessitates the removal and/or recharging of such immobilized solids. The synthesis of nanoparticles[31−34] can mitigate clogging caused by flow-induced bridging but can lead to retention and build-up when the particles interact with the surfaces of the system. Another approach is to use multiphase liquid−liquid flow to prevent particles from interacting with the walls of the microchannels. Encapsulating particles in droplets[21,23,28] or establishing annular-type flow[30] not only limits the interactions between the particles and walls but also constrains particle-to-particle interactions that may lead to clogging. However, these specialized systems often require the use of solvents that can be incompatible with certain reagents or can lead to changes in the efficiency of many organic reactions. Noninvasive approaches such as flow focusing and filtration have proven to

* To whom correspondence should be addressed. E-mail: kfjensen@mit.edu. Tel: +1 617 253-4589. Fax: +1 617 298-8992.
† Department of Chemical Engineering.
‡ Department of Chemistry.

(1) Roberge, D. M.; Ducry, L.; Bieler, N.; Cretton, P.; Zimmermann, B. *Chem. Eng. Technol.* **2005**, *28*, 318–323.
(2) Carey, J. S.; Laffan, D.; Thomson, C.; Williams, M. T. *Org. Biomol. Chem.* **2006**, *4*, 2337–2347.
(3) Dugger, R. W.; Ragan, J. A.; Ripin, D. H. B. *Org. Process Res. Dev.* **2005**, *9*, 253–258.
(4) Jensen, K. F. *Chem. Eng. Sci.* **2001**, *56*, 293–303.
(5) Fletcher, P. D. I.; Haswell, S. J.; Pombo-Villar, E.; Warrington, B. H.; Watts, P.; Wong, S. Y. F.; Zhang, X. L. *Tetrahedron* **2002**, *58*, 4735–4757.
(6) Jahnisch, K.; Hessel, V.; Lowe, H.; Baerns, M. *Angew. Chem., Int. Ed.* **2004**, *43*, 406–446.
(7) Pennemann, H.; Watts, P.; Haswell, S. J.; Hessel, V.; Lowe, H. *Org. Process Res. Dev.* **2004**, *8*, 422–439.
(8) Hessel, V.; Lowe, H. *Chem. Eng. Technol.* **2005**, *28*, 267–284.
(9) Jensen, K. F. *MRS Bull.* **2006**, *31*, 101–107.
(10) deMello, A. *J. Nature* **2006**, *442*, 394–402.
(11) Mason, B. P.; Price, K. E.; Steinbacher, J. L.; Bogdan, A. R.; McQuade, D. T. *Chem. Rev.* **2007**, *107*, 2300–2318.
(12) Watts, P.; Wiles, C. *Chem. Commun.* **2007**, 443–467.
(13) Watts, P.; Wiles, C. *Chem. Eng. Technol.* **2007**, *30*, 329–333.
(14) Hartman, R. L.; Jensen, K. F. *Lab Chip* **2009**, *9*, 2495–2507.
(15) Ehrfeld, W.; Hessel, V.; Lowe, H. *Microreactors: New Technology for Modern Chemistry*; Wiley-VCH: Weinheim, Germany, 2000.
(16) Jensen, K. F. In *New Avenues to Efficient Chemical Synthesis: Emerging Technologies*; Seeberger, P. H., Blume, T., Eds.; Springer-Verlag: Berlin, Heidelberg, 2007; p 5776.
(17) Haswell, S. J.; O'Sullivan, B.; Styring, P. *Lab Chip* **2001**, *1*, 164–166.
(18) Losey, M. W.; Schmidt, M. A.; Jensen, K. F. *Ind. Eng. Chem. Res.* **2001**, *40*, 2555–2562.
(19) Baxendale, I. R.; Deeley, J.; Griffiths-Jones, C. M.; Ley, S. V.; Saaby, S.; Tranmer, G. K. *Chem. Commun.* **2006**, 2566–2568.
(20) Wiles, C.; Watts, P.; Haswell, S. *J. Lab Chip* **2007**, *7*, 322–330.
(21) Poe, S. L.; Cummings, M. A.; Haaf, M. R.; McQuade, D. T. *Angew. Chem., Int. Ed.* **2006**, *45*, 1544–1548.
(22) Kockmann, N.; Kastner, J.; Woias, P. *Chem. Eng. J.* **2008**, *135*, S110–S116.
(23) Song, H.; Chen, D. L.; Ismagilov, R. F. *Angew. Chem., Int. Ed.* **2006**, *45*, 7336–7356.
(24) Horie, T.; Sumino, M.; Tanaka, T.; Matsushita, Y.; Ichimura, T.; Yoshida, J. *Org. Process Res. Dev.* **2010**, *14*, 405–410.
(25) Conant, T.; Karim, A.; Rogers, S.; Samms, S.; Randolph, G.; Datye, A. *Chem. Eng. Sci.* **2006**, *61*, 5678–5685.
(26) Li, W.; Pharn, H. H.; Nie, Z.; MacDonald, B.; Guenther, A.; Kumacheva, E. *J. Am. Chem. Soc.* **2008**, *130*, 9935–9941.
(27) Kobayashi, J.; Mori, Y.; Okamoto, K.; Akiyama, R.; Ueno, M.; Kitamori, T.; Kobayashi, S. *Science* **2004**, *304*, 1305–1308.
(28) Shestopalov, I.; Tice, J. D.; Ismagilov, R. F. *Lab Chip* **2004**, *4*, 316–321.
(29) Trachsel, F.; Tidona, B.; Desportes, S.; Rudolf von Rohr, P. *J. Supercrit. Fluids* **2009**, *48*, 146–153.
(30) Nagasawa, H.; Mae, K. *Ind. Eng. Chem. Res.* **2006**, *45*, 2179–2186.
(31) Takagi, M.; Maki, T.; Miyahara, M.; Mae, K. *Chem. Eng. J.* **2004**, *101*, 269–276.
(32) Khan, S. A.; Jensen, K. F. *Adv. Mater.* **2007**, *19*, 2556.
(33) Khan, S. A.; Gunther, A.; Schmidt, M. A.; Jensen, K. F. *Langmuir* **2004**, *20*, 8604–8611.
(34) Yen, B. K. H.; Gunther, A.; Schmidt, M. A.; Jensen, K. F.; Bawendi, M. G. *Angew. Chem., Int. Ed.* **2005**, *44*, 5447–5451.

10.1021/op100154d
Published on Web 09/10/2010

be effective in separating particles based on hydrodynamic conditions.[35−38] These conditions, however, limit reaction screening applications and present challenges with systems that have high particle concentrations or particles that have an affinity for each other or the surfaces of the reactor. Electrical potentials have also been used to sort particles in microfluidic systems.[39,40] Yet another noninvasive approach is the application of acoustic standing waves to order particles, such as the acoustic streaming of blood cells.[41−44] More recently, we have demonstrated the potential for using ultrasound to handle solids during the course of a chemical reaction, while others have combined ultrasound and multiphase flow to facilitate the flow of solids during polymerization.[24] In general, the strategy for solids handling depends on the nature of the chemistry and warrants a deeper understanding of the mechanisms that lead to clogging.

The Pd-catalyzed C−N bond forming reaction is one of the most important reactions of the past 15 years, finding applications in the production of APIs, natural products, and specialty chemicals.[45−48] It is a versatile transformation that allows the coupling of aryl and vinyl halides, triflates, nonaflates, and other sulfonates with a wide variety of nitrogen nucleophiles. These reactions, and many others used in fine chemical production, form inorganic salt byproducts and are often run in nonpolar solvents, which leads to precipitation.

In the present work, we use the Pd-catalyzed amination reaction to investigate the mechanisms that govern the clogging of microreactors.[49] We will show that both bridging and constriction are important mechanisms that lead to clogging and serve to limit the application of microsystems to reactions that form insoluble byproducts. We present several approaches to overcome the challenge of plugging and thus enable continuous-flow microchemical synthesis of a biaryl amine. Consequently, the present work establishes the groundwork for further continuous-flow studies on both the mechanisms responsible for clogging and synthetic applications of Pd-catalyzed cross-coupling reactions.

2. Reactor Design

2.1. Microfabrication and Materials. Microchannel devices were fabricated from a double-side-polished silicon wafer and capped with a Pyrex wafer. As shown in Figure 1a, the fabrication process involved several photolithography steps, deep reactive ion etching of the silicon, and growth of a low-stress silicon nitride coating (0.5 μm). Anodic bonding of the Pyrex wafer capped the etched silicon-nitride-coated features and completed the microfluidic device. The packaged device, with a serpentine microchannel (0.4 × 0.4 × 875 mm) is shown in Figure 1b. As will be discussed later, a device with a spiral microchannel, of the same dimensions, was also fabricated in the same manner (Figure 1c). The halo through-etch between the cooled inlets and outlet and main channel (Figure 1b) provided thermal separation between the two parts of the reactor and allowed for operation with two separate temperature zones, each nearly isothermal, on a single chip.[34] High purity polytetrafluoroethylene (PFA) capillaries were also found to be useful as model reactors (Figure 1d).

2.2. Acoustic Integration and Layout. Figure 2a illustrates the equipment configuration used for the present study. Reagents in 10 mL glass syringes were delivered to the microreactor (see Figure 1B) by syringe pumps. A stainless-steel pressure transducer was plumbed directly into one of the reagent lines upstream to the mixing point. It was possible to constantly monitor the pressure entering the reactor. Upon exiting the reactor, the mixture passed through approximately 120 μL of PFA tubing at ambient temperature before it was collected in a vial that was under a constant 1.7 psig pressure of argon. Experiments with acoustic irradiation were performed by replacing the microreactor of Figure 1b with lengths of loosely coiled PFA tubing ($^1/_{16}$ in. o.d., 500 or 1000 μm i.d.) (Figure 2b). Upon exiting the bath, the reaction mixture was collected under argon as described above.

3. Results and Discussion

In this study of clogging on the microscale, we employed the coupling of 4-chloroanisole and aniline, catalyzed by catalyst supported by one of the bulky, electron-rich, biaryl phosphine ligands, to form 4-methoxy-*N*-phenylaniline (Scheme 1).[50]

It can be seen in Scheme 1 that sodium chloride is formed as a stoichiometric byproduct in this reaction. Inorganic salts are generally insoluble in the solvents used to carry out this reaction (e.g., 1,4-dioxane, toluene, THF). To complicate matters further, typical batch conditions for these reactions employ high concentrations (0.5−1.0 M) and the reactions are often complete in minutes, resulting in fast rates of salt formation. This is a problem that is synthetically interesting, yet challenging to carry out under flow conditions; it served as a model to study solids handling in microsystems.

(35) Di Carlo, D.; Irimia, D.; Tompkins, R. G.; Toner, M. *P. Natl. Acad. Sci. U.S.A.* **2007**, *104*, 18892–18897.
(36) Yamada, M.; Seki, M. *Lab Chip* **2005**, *5*, 1233–1239.
(37) Kuntaegowdanahalli, S. S.; Bhagat, A. A. S.; Kumar, G.; Papautsky, I. *Lab Chip* **2009**, *9*, 2973–2980.
(38) Huang, L. R.; Cox, E. C.; Austin, R. H.; Sturm, J. C. *Science* **2004**, *304*, 987–990.
(39) Kralj, J. G.; Lis, M. T. W.; Schmidt, M. A.; Jensen, K. F. *Anal. Chem.* **2006**, *78*, 5019–5025.
(40) Pamme, N. *Lab Chip* **2007**, *7*, 1644–1659.
(41) Laurell, T.; Petersson, F.; Nilsson, A. *Chem. Soc. Rev.* **2007**, *36*, 492–506.
(42) Nilsson, A.; Petersson, F.; Jonsson, H.; Laurell, T. *Lab Chip* **2004**, *4*, 131–135.
(43) Petersson, F.; Aberg, L.; Sward-Nilsson, A. M.; Laurell, T. *Anal. Chem.* **2007**, *79*, 5117–5123.
(44) Petersson, F.; Nilsson, A.; Holm, C.; Jonsson, H.; Laurell, T. *Lab Chip* **2005**, *5*, 20–22.
(45) Surry, D. S.; Buchwald, S. L. *Angew. Chem., Int. Ed.* **2008**, *47*, 6338–6361.
(46) Buchwald, S. L.; Jiang, L. In *Metal-Catalyzed Cross-Coupling Reactions*; deMeijere, A, Diederich, F., Eds.; Wiley-VCH: Weinheim, 2004; p 699.
(47) Hartwig, J. F. *Acc. Chem. Res.* **2008**, *41*, 1534–1544.
(48) Marion, N.; Nolan, S. P. *Acc. Chem. Res.* **2008**, *41*, 1440–1449.
(49) For references pertaining to palladium-catalyzed amination reactions in microflow see: Mauger, C.; Buisine, O.; Caravieilhes, S.; Mignani, G. *J. Organomet. Chem.* **2005**, *690*, 3627–3629. Murphy, E. R.; Martinelli, J. R.; Zaborenko, N.; Buchwald, S. L.; Jensen, K. F. *Angew. Chem., Int. Ed.* **2007**, *46*, 1734–1737. Popa, D.; Marcos, R.; Sayalero, S.; Vidal-Ferran, A.; Pericàs, M. A. *Adv. Synth. Catal.* **2009**, *351*, 1539–1556. Shore, G.; Morin, S.; Mallik, D.; Organ, M. G. *Chem.—Eur. J.* **2008**, *14*, 1351–1356. Bazinet, P.; McMullen, J. P.; Naber, J. R.; Musacchio, A.; Jensen, K. F.; Buchwald, S. L.; *Angew. Chem., Int. Ed.*, submitted for publication. Naber, J. R.; Buchwald, S. L. *Angew. Chem., Int. Ed.*, submitted for publication.
(50) Huang, X.; Anderson, K. W.; Zim, D.; Jiang, L.; Klapars, A.; Buchwald, S. L. *J. Am. Chem. Soc.* **2003**, *125*, 6653–6655.

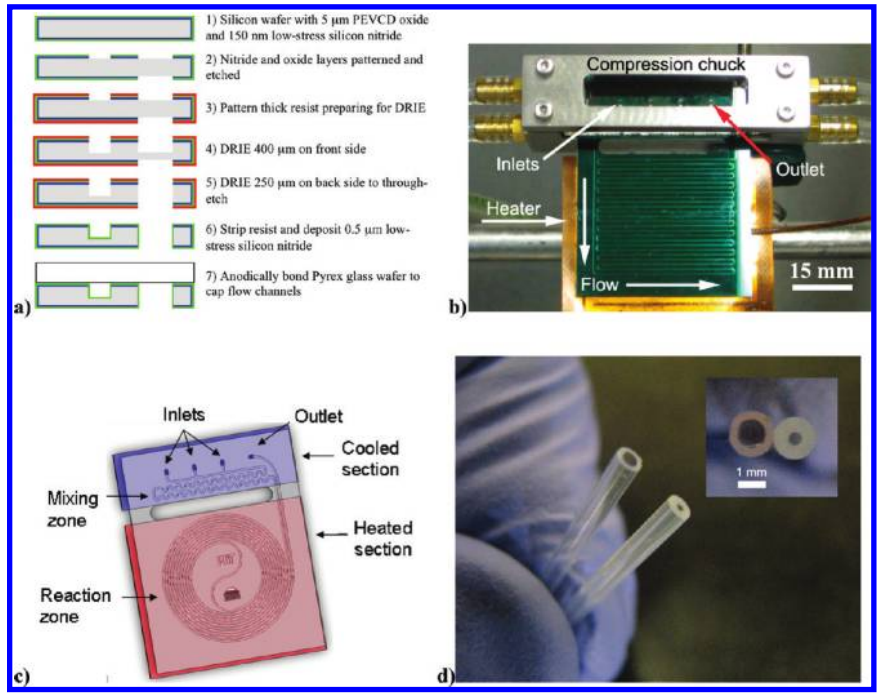

Figure 1. **(a) Microreactor fabrication process. (b) Silicon microreactor with serpentine channels used to study solids handling. The image shows a compression chuck used to cool the inlets and outlet of each device. (c) Silicon microreactor designed to eliminate the 180° turns. The device has a gradual spiral in and out to imitate a long straight channel. (d) PFA capillaries used as model reactors (i.d. = 500 and 1000 μm).**

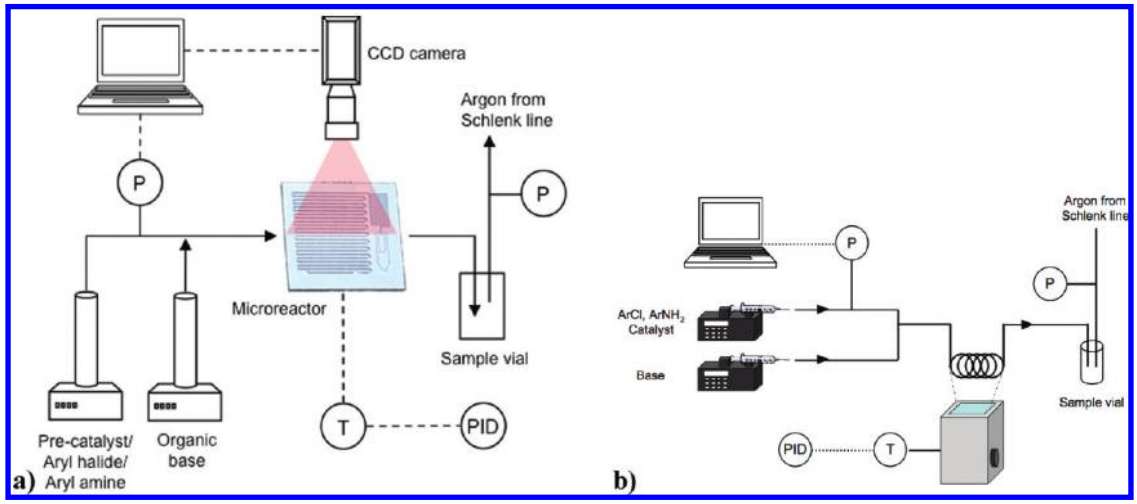

Figure 2. **Experimental setup used to carry out solids handling experiments: (a) a silicon-based microreactor; (b) PFA capillary in an ultrasonic bath.**

Scheme 1. **Pd-Catalyzed amination of an aryl chloride with aniline**

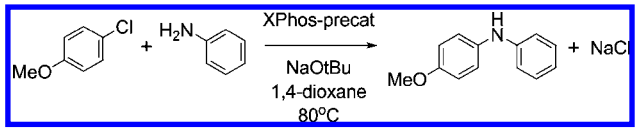

3.1. Clogging Mechanisms. The aforementioned reaction was first carried out in a series of experiments using a silicon-based microreactor to allow the process to be followed visually. Figure 3a shows that the dimensionless pressure drop across the microreactor, $\Delta P/\Delta P_0$ (normalized to the initial, solvent-only, pressure drop), rapidly increased upon injecting the reagents at 20 μL/min (τ = 7 min) and 80 °C, even when the concentration of aryl halide was only 0.1 M (concentrations refer to the reaction mixture after the two streams are combined). The sudden increase in pressure drop was followed by clogging of the microreactor to the point that no flow occurred. As evident in Figure 3a, the onset of clogging took place after less than 6 reactor volumes injected.

As shown in Figure 3b, clogging was caused by a white solid that accumulated at the 180° turns within the microreactor. Under increased magnification (Figure 3c) it can be seen that the solid material was crystalline in nature and the sizes of the particles found were on the same order as the channel dimensions (e.g., 400 μm). Here, we define the crystal size as the largest cross-section dimension of an individual particle. When the size of flowing and stable particles is on the order of the cross-sectional length of a channel, it has been shown that bridging takes place in micrometer-sized pore throats[51−53] and fabricated geometries.[54] The depiction in Figure 3d illustrates

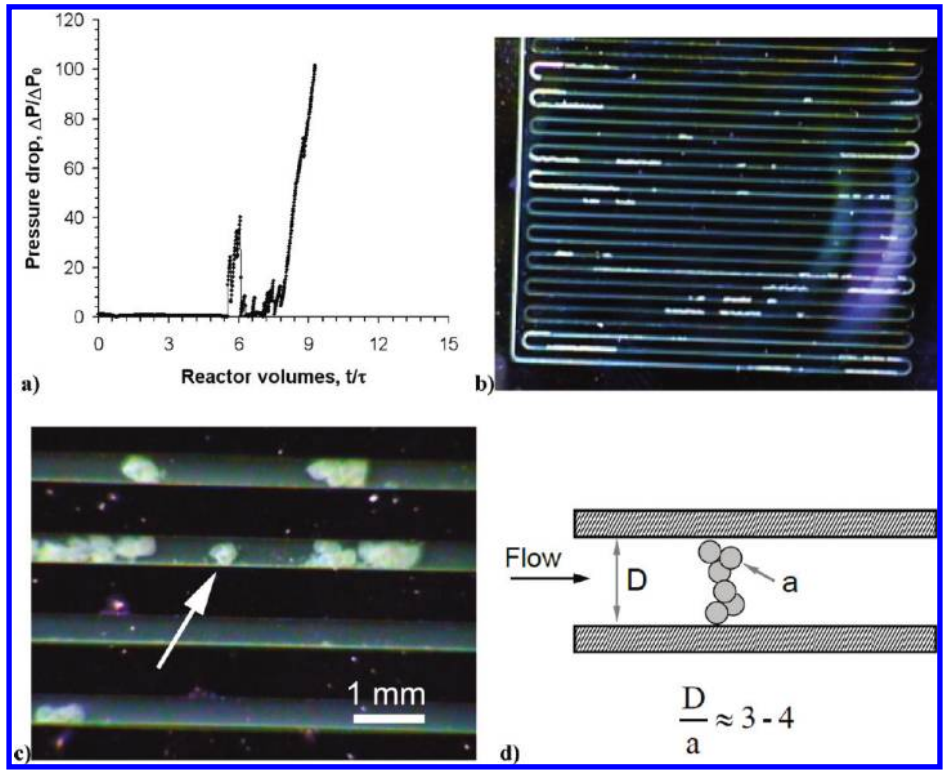

Figure 3. **Pd-catalyzed amination leading to bridging in microreactors. (a) Dimensionless pressure drop across a microreactor during the injection of the reagents and catalyst (at 20 μL/min and 80 °C) shown in Scheme 1. (b) Photograph of the microreactor illustrating the accumulation of white solid, primarily at 180° turns. (c) Expanded view of the microchannel. (d) Depiction of flow-induced bridging between two flat plates.**

that particles can plug by forming a bridge across a microchannel. It is generally understood that particles can be retained when the aspect ratio (e.g., the ratio of channel width to particle size, D/a, is in the range 3−4.[51] It should be noted, however, that this type of bridging has been shown for stable particle suspensions that do not exhibit attractive interactions or that do not change size with time. Based on our experimental observations, it is evident that bridging also takes place during the amination reaction and is one of the mechanisms that leads to clogging.

The clogged microreactor was replaced with a fresh device and the reaction was repeated with an increased injection rate of 70 μL/min (τ = 2 min). Figure 4a shows that the pressure drop once again increased to the point of clogging with the injection of only a few reactor volumes of the reaction. However, in this case the pressure drop gradually increased for 4 reactor volumes before suddenly rising and clogging.

Further inspection of the microreactor (Figure 4b) illustrates that the reactor walls changed color, implying that material was deposited or grown on these surfaces. Both deposition[55−57] and nucleation followed by growth can lead to channel constriction (Figure 4c). A time-dependent decrease in cross-sectional diameter will likely bring about bridging in a system with particles suspended in the bulk solution. The presence of constriction in addition to bridging warrants more than one approach to address the clogging issues caused by the insoluble byproducts of the Pd-catalyzed amination.

3.2. Influence of Reactor Geometry. Particle-to-wall interactions can take place in laminar flow when changes in the velocity occur (e.g., fluid flow around turns) or when the particle momentum is too large for particles to stay on a streamline path (e.g., inertial impaction).[55] To minimize these scenarios, we investigated the use of silicon microreactors with gradual turns (e.g., analogous to coiled tubing), as shown in Figure 1c. The reactor design was closely related to the serpentine microreactor (Figure 1b), retaining the same layout of ports and mixing zone, an equal volume, and an identical thermal isolation of the reaction zone from the ports. However, the nested spiral layout of the heated channel provided a gradual change in turning radius, with the sharpest turn having a much larger radius (4.4 mm) than the hairpin turns (0.4 mm) of the serpentine layout. When the experiment described in Figure 3 was repeated using the spiral reactor, we observed the solids flowed for several reactor volumes without the accumulation shown in Figure 3b. Nevertheless, the microreactor wall (from the top down) gradually changed from transparent to white, and clogging eventu-

(51) Ramachandran, V.; Fogler, H. S. *J. Fluid Mech.* **1999**, *385*, 129–156.
(52) Vitthal, S.; Sharma, M. M. *J. Colloid Interface Sci.* **1992**, *153*, 314–336.
(53) Muecke, T. W. *J. Petrol. Tech.* **1979**, *31*, 144–150.
(54) Wyss, H. M.; Blair, D. L.; Morris, J. F.; Stone, H. A.; Weitz, D. A. *Phys. Rev. E Stat. Nonlin. Soft. Matter Phys.* **2006**, *74*, 061402.
(55) Ramachandran, V.; Fogler, H. S. *Langmuir* **1998**, *14*, 4435–4444.
(56) Song, L. F.; Elimelech, M. *J. Colloid Interface Sci.* **1994**, *167*, 301–313.
(57) Marshall, J. K.; Kitchener, J. A. *J. Colloid Interface Sci.* **1966**, *22*, 342–351.

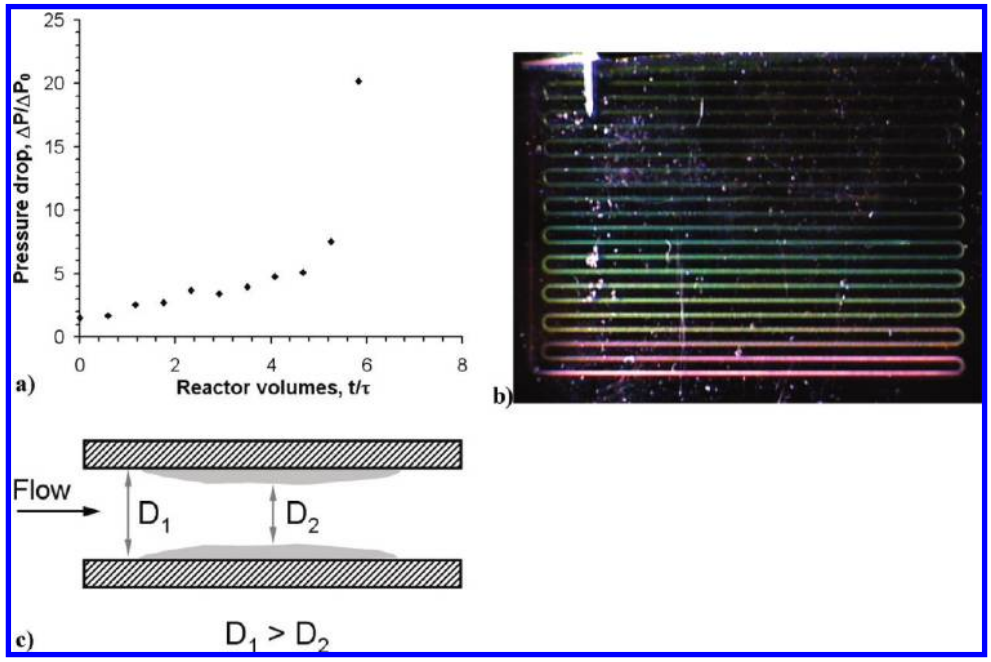

Figure 4. **Pd-catalyzed amination resulting in constriction in a microreactor. (a) Dimensionless pressure drop across a microreactor during the injection of the reagents and catalyst (at 70 μL/min and 80 °C) shown in Scheme 1. (b) Photograph of the microreactor during reaction. (c) Depiction of constriction when material grows or deposits on a channel wall.**

ally took place. A video of these results can be found in the Supporting Information.

3.3. Acoustic Irradiation. It is commonly known that sound waves can impose a force on a system of particles.[58] Thus, we investigated the influence of acoustic waves on microreactor clogging during Pd-catalyzed C−N bond forming reactions. In the case of a standing wave, the amplitude of the primary radiation force acting on a particle (in the radial direction) flowing in a microchannel, F_r, has previously been described and given as[41,42]

$$F_r = -\left(\frac{2\pi^2 p_0^2 r^3 \beta_S}{3\lambda}\right) \cdot \phi \cdot \sin\left(\frac{4\pi x}{\lambda}\right) \qquad (1)$$

where p_0 is the acoustic pressure amplitude, r is the particle radius, β_S is the compressibility of the solvent, and ϕ is a contrast factor, described as[41,42]

$$\phi = \left(\frac{5\rho_P - 2\rho_S}{2\rho_P + \rho_S}\right) - \frac{\beta_P}{\beta_S} \qquad (2)$$

where ρ is density, and the subscripts P and S denote the particle and solvent, respectively. One observes in eq 1 that the primary force is strongly dependent on particle radius; thus, the acoustic force weakens as the particle diameter is reduced. Furthermore, the primary force is driven by differences in density and compressibility, described by the contrast factor. The acoustic pressure amplitude also influences the primary radiation force and is dependent on the voltage and frequency under which piezoceramic operation takes place. Such forces have been exploited to order and separate particulates and biological matter when frequencies are in the range of megahertz and wavelengths are on the order of the channel dimensions.[41,42,59,60] We wanted to study whether these forces, with frequencies in the kilohertz range, could be used to overcome the particle-to-particle attractive interactions and hydrodynamic conditions that bring about bridging in laminar flow (see the Supporting Information for a description of the acoustic waveform applied in this study).

The reaction from Scheme 1 was carried out both with and without acoustic irradiation by injecting the reagents and base (0.1 M ArCl, $\tau = 7$ min) into a PFA capillary (1000 μm i.d., 240 μL) coiled in an ultrasonic bath filled with water at 80 °C. Figure 5a shows that the microreactor clogged in the absence of ultrasound, shown by the rapid increase in dimensionless pressure drop. Repeating the experiment with acoustic irradiation demonstrated that the presence of ultrasound prevented clogging, as the pressure drop remained negligible for approximately 20 reactor volumes. Removing the acoustic irradiation in the same experiment resulted in clogging of the microreactor, as shown in Figure 5a, and subsequent investigations proved that reinitiating the ultrasonic bath did not unplug the reactor.

The effect of channel dimensions on plugging was examined by repeating the experiment described in Figure 5a with a smaller capillary (500 μm i.d.). The reactor volume (240 μL) and injection rate ($\tau = 7$ min) were held constant by increasing the reactor length. As shown in Figure 5b, the dimensionless pressure drop also remained small until the acoustic irradiation was removed. In both cases, samples were collected, and yield and conversion, relative to the internal standard, were determined by GC to be 100% and >95%, respectively. Given that the reaction rate increases with concentration we investigated whether acoustic-mediated transport would allow for uninter-

(58) Mason, W. P. *Physical Acoustics*; Academic Press: New York, 1982. Challis, R. E.; Povey, M. J. W.; Mather, M. L.; Holmes, A. K. *Rep. Prog. Phys.* **2005**, *68*, 1541–1637. Gedanken, A. *Ultrason. Sonochem.* **2004**, *11*, 47–55. Spengler, J.; Jekel, M. *Ultrasonics* **2000**, *38*, 624–628.

(59) Coakley, W. T. *Trends Biotechnol.* **1997**, *15*, 506–511.

(60) Hawkes, J. J.; Barber, R. W.; Emerson, D. R.; Coakley, W. T. *Lab Chip* **2004**, *4*, 446–452.

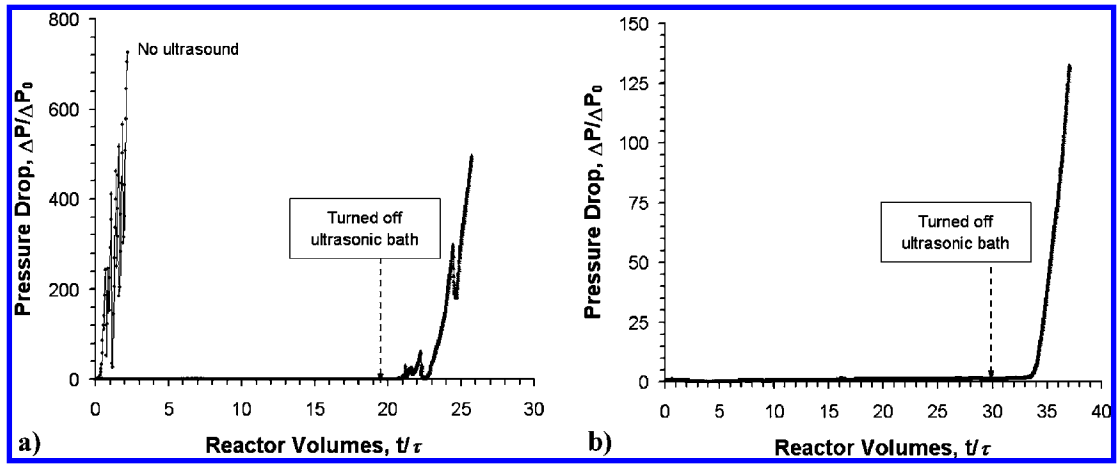

Figure 5. **(a) Dimensionless pressure drop during the reaction (τ = 7 min, 0.1 M ArCl) in a PFA capillary (1000 μm i.d., 240 μL) at 80 °C. The figure illustrates that the presence of acoustic forces prevents the pressure drop from rapidly increasing. (b) Repeating the same experiment with 500 μm PFA tubing revealed a similar result.**

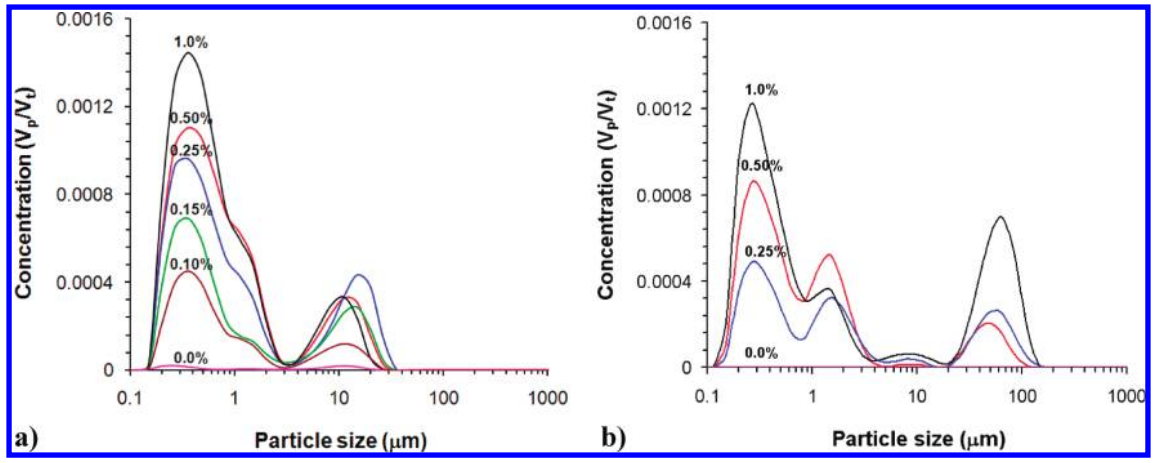

Figure 6. **(a) Particle size estimation for the reaction in the presence of ultrasound. (b) Particle size estimation for the reaction in the absence of ultrasound. The figures show that acoustic irradiation reduces the maximum effective particle size; the larger particles are likely aggregates.**

rupted flow when concentrations were closer to those of traditional batch experiments (e.g., 1 M). However, we found that the solubility limit of NaO*t*-Bu in 1,4-dioxane at room temperature was approximately 1.0 M. Taking into account both the stoichiometry of the reaction and the dilution resulting from the combination of the base stream and the stream containing the remainder of the reagents, the maximum concentration was determined to be 0.36 M in ArCl. Under these conditions (τ = 1 min), flow was possible in the presence of ultrasound, samples were collected, and the conversion and yield were measured to be 100% and >95% by GC, relative to the internal standard. These observations were made for both 500 and 1000 μm PFA microreactors. Nevertheless, exactly why the ultrasound was preventing clogging remained ambiguous.

To elucidate the role of acoustic irradiation on flow, particles exiting the capillary (1000 μm i.d., τ = 1 min) were analyzed. The reaction mixture was collected into vials, under an argon atmosphere, containing 1,4-dioxane and the samples were analyzed using a laser diffraction analyzer. Reactions were run with catalyst loadings increasing from 0 to 1.0 mol % to give increasing conversions and yields without changing the flow conditions or the reagent concentrations of the experiments. As evident in Figure 6a, varying the catalyst loading (in separate experiments) yielded particles ranging in diameter from approximately 0.15 to 36 μm. The different loadings resulted in different total particle concentrations (depending on the reaction conversion); however, the relative particle size distributions were equivalent in all cases.

In a separate set of experiments, we were able to flow the reaction for several reactor volumes in the absence of ultrasound without plugging. Samples were collected before plugging took place, and particle size analysis revealed particles in the range 0.15−112 μm, as shown in Figure 6b. The additional mode of particles observed in Figure 6b can be attributed to the aggregation of the salt particles, and combination of the results in Figure 6a,b demonstrates that ultrasonic forces can reduce the effective maximum particle size, which in turn prevents bridging. Thus, applying external forces such as ultrasonic irradiation can influence and even overcome the particle-to-particle interactions that can lead to clogging via bridging. In general, mixing can influence the distributions of particle sizes in microscale reactors[61] and may be different from those measured in batch vessels. As we have seen, the presence of acoustics can lead to different particle sizes. One might, therefore, consider the overall influence of acoustics and reactor

(61) Yen, B. K. H. Massachusetts Institute of Technology, 2007.

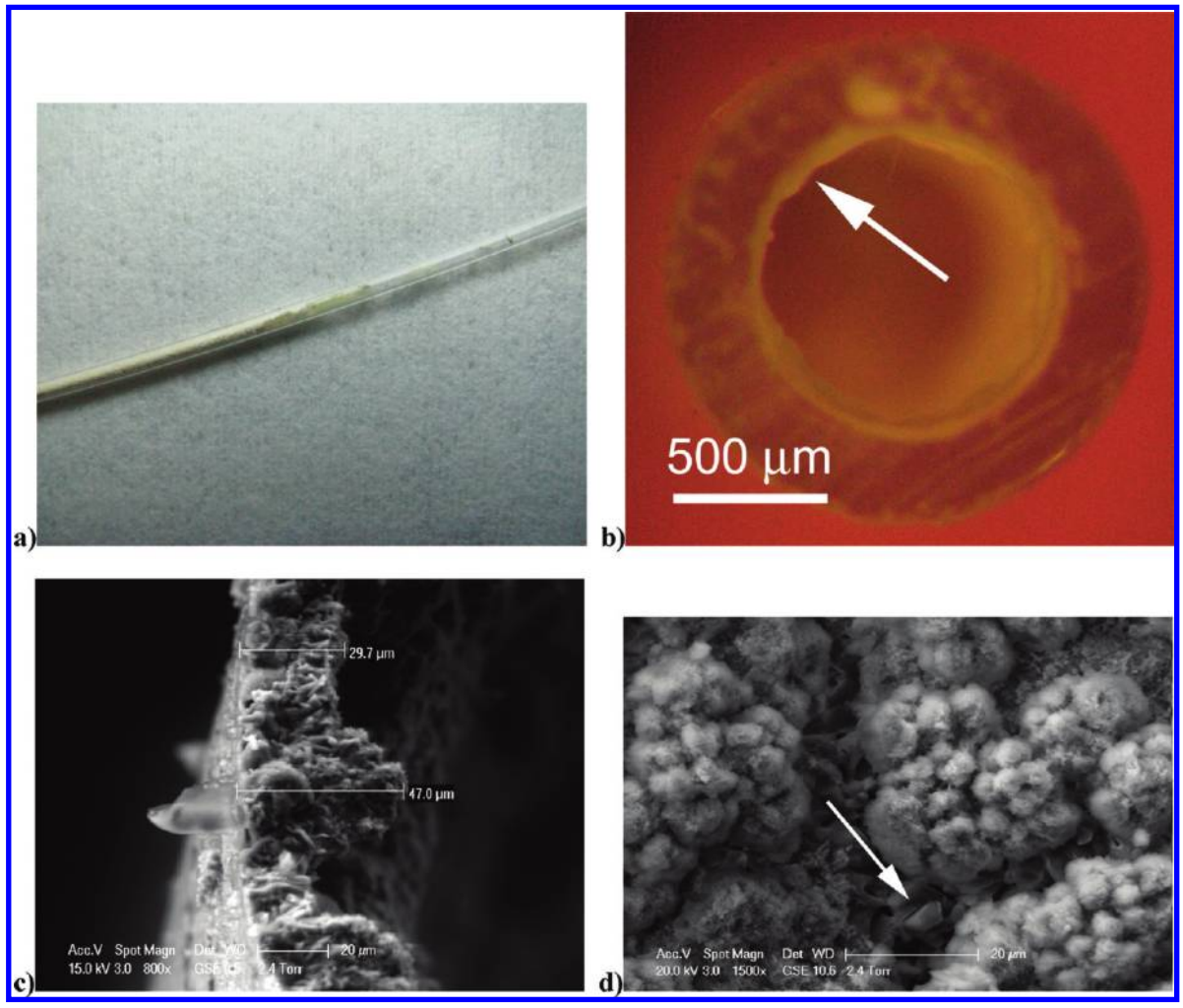

Figure 7. **(a) PFA capillary showing the wall deposit (left side) after the reaction mixture exited the heated section exposed to acoustics (right side). (b) Cross-section of the capillary illustrating the wall deposit. SEM micrographs of the wall deposit in the (c) axial and (d) radial direction.**

design (e.g., batch or tubular) on the expected particle size if it is relevant to a particular process.

The experimental results shown in Figure 6a,b offer insight on potential microreactor designs that could prevent bridging for Pd-catalyzed aminations or other salt forming reactions. From Figure 6a, the experiment in the presence of ultrasound, the aspect ratio (D/a) between the largest particle and the capillary (1000 μm i.d.) was 28. Without any ultrasound, Figure 6b, the system clogged even though the aspect ratio of 8.9 was greater than the previously stated cutoff of 4 that has been determined for stable colloids.[51] Attractive particle interactions likely contributed to clogging at this aspect ratio. Nevertheless, these observations imply that microreactors with channels of 400 μm could potentially tolerate NaCl particles in the range of 14 μm without bridging. It is possible, however, that particles larger than 14 μm but smaller than 45 μm (i.e., aspect ratio of 8.9) will not bridge. However, these conservative approximations neglect the time-dependent change in microchannel geometry caused by constriction via particle deposition or growth.

3.4. Constriction via Deposition or Growth. As shown in the microreactor of Figure 4, constriction can take place in addition to bridging. Switching the reactor surface from silicon nitride to fluoropolymer did not inhibit constriction, as white material gradually formed on the PFA capillary walls after injecting approximately 40 reactor volumes. It should be noted, however, that this material was observed to form upon the walls of the tubing after the heated zone where the exposure to ultrasound was limited. No wall deposits were observed to form in the section of the reactor exposed to ultrasound. Parts a and b of Figure 7 illustrate the axial and radial cross-sections, respectively, of the capillary containing the wall deposits. The capillary was filled with reaction solvent (1,4-dioxane) and was cooled below the freezing point of the solvent (11.8 °C). Cuts were immediately made with a razor to preserve the deposited material on the capillary walls.

Examination of these deposits with scanning electron microscopy illustrated the film thickness to range from 30 to 50 μm (Figure 6c). As shown in Figure 7d, the deposit was composed of cauliflower-type clusters, which could be particle aggregates. Further inspection of the film with SEM revealed the presence of different crystals, highlighted in Figure 7d. X-ray diffraction later confirmed the material to be a composite of sodium chloride and an unknown organic crystal (see Supporting Information). Isolation and GCMS analysis of this unknown substance revealed that it is at least, in part, reaction product. Subsequent experiments proved that the deposited material could be easily removed by flushing with reaction solvent

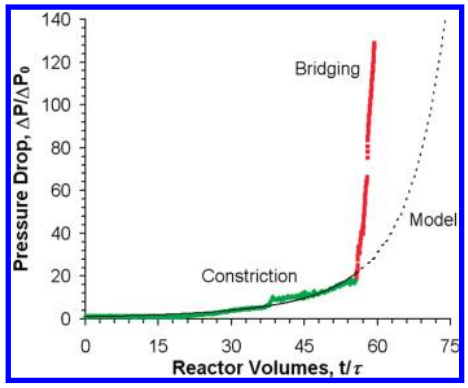

Figure 8. **Dimensionless pressure drop during the reaction (τ = 3 min, 0.36 M ArCl) in a PFA capillary (1000 μm i.d., 240 μL) at 80 °C. The experimental data are plotted with the model of eq 4, illustrating that constriction initially took place, followed by bridging.**

followed by water. In this case, constriction could be managed via periodic flushing schemes, especially when the deposition or growth rate is predictable.

When constriction takes place before heating of the reactants or after they have been cooled, the concentration of starting material or the particles formed remains relatively constant. It is under these conditions that the change in microchannel geometry is a constant, α, and expressed as

$$\frac{dD}{dt} = -\alpha \tag{3}$$

A reduction in cross-section diameter is readily monitored by measurement of the pressure drop. For laminar flow in a cylindrical pipe, it can be shown that

$$\frac{\Delta P}{\Delta P_0} = \frac{1}{(1 - \gamma t^*)^4} \tag{4}$$

when

$$\gamma = \frac{\alpha \tau}{D_0} \tag{5}$$

and

$$t^* = \frac{t}{\tau} \tag{6}$$

where D_0 is the initial channel diameter, D is the diameter at time t, and τ is the residence time.

Equation 4 can be applied to approximate a constriction rate, α, or to determine the clogging mechanism. When constriction takes place, one would expect the dimensionless pressure drop to gradually increase before plugging, as was the case in Figure 4. Repeating an experiment in a 1000 μm capillary (240 μL and τ = 3 min) in the presence of acoustics and expanding the y-axis revealed an important observation. As can be seen in Figure 8, an abrupt increase took place after injecting 57 reactor volumes, while the approximation of eq 4 predicts the pressure increase at a later time. These results imply that constriction of the microreactor diameter eventually resulted in bridging. From eq 5, the constriction rate was estimated to be 3.2 μm/min. Assuming that the particles had stopped growing (i.e., only particle aggregation took place), we can predict from Figure 6a and a constriction rate of 3.2 μm/min that the bridging took place when particles were in the range of 16 μm.

3.5. Eliminating Bridging and Constriction. The rate at which salt byproduct accumulates on the surface is influenced by convection. To examine this influence, the experiment of Figure 8 was repeated, and the total reactor volume increased from 240 to 600 μL while maintaining a constant residence time of 3 min. The reactor volume exiting the ultrasonic bath was also held constant at 120 μL. One observes in Figure 9a that increasing the flow rate from 80 μL/min (average velocity v_{avg} = 10.2 cm/min) to 200 μL/min (v_{avg} = 25.5 cm/min) decreased the constriction rate. The solid curved lines of Figure 9a represent eq 4. Applying eqs 4 and 5 yields a constriction rate of approximately 1.8 μm/min upon increasing the flow rate to 200 μL/min. These observations demonstrate that convective forces alone can potentially overcome the particle-to-particle or particle-to-wall interactions that lead to constriction. Moreover, the particles can interact mechanically with the deposit and limit growth via abrasion. Partial evidence of this phenomenon can be seen in Figure 9b. Before bridging, the pressure drop appeared to approach a plateau (see Figure 9b). Reducing the residence time from 3 to 1 min eliminated constriction and bridging altogether, despite the reaction being complete in all cases. Consequently, the dimensionless pressure drop remained approximately 1 even after injecting 76 reactor volumes.

3.6. Influence of Acoustics on Reaction. Ultrasound has proven to be a useful tool in enhancing the rate of organic transformations,[62,63] including reactions catalyzed by palladium.[64] It is generally understood that the energy emitted from cavitations can contribute to enhanced reaction rates in batch-scale systems that have temperature gradients. Recently, the research work of others has elucidated that ultrasound enhances mixing in microfluidic systems.[60,65,66] We questioned whether these temperature and mixing effects would impact the Pd-catalyzed C−N bond formation reaction in capillary flow.

The coupling reaction was carried out in a PFA capillary at 80 °C and a residence time of 1 min. As shown in Figure 10, increasing the catalyst loading from 0−1.0 mol % resulted in increased conversion from starting material to the biaryl amine product. Without any ultrasound, the yield was reduced for a given catalyst loading. The data in Table 1 show the results of a series of experiments performed to confirm the results in Figure 10. Solution 1 (1.0 M NaOtBu in 1,4-dioxane) and solution 2 (0.72 M ArCl, 0.86 M aniline, 0.14 M biphenyl, and 3.6 mM XPhos precatalyst in 1,4-dioxane) were injected (120 μL/min each, τ = 1 min) into a PFA capillary ($^1/_{16}$ in. o.d., 1000 μm i.d., 240 μL heated, 360 μL total) submerged in an ultrasonic bath filled with water at 80 °C. While sonicating, the reaction was run for 5 min to achieve steady state, at which point sample 1 was collected (5 reactor volumes). The sonication

(62) Thompson, L. H.; Doraiswamy, L. K. *Ind. Eng. Chem. Res.* **1999**, *38*, 1215–1249.
(63) Mason, T. *J. Chem. Soc. Rev.* **1997**, *26*, 443–451.
(64) Barge, A.; Tagliapietra, S.; Tei, L.; Cintas, P.; Cravotto, G. *Curr. Org. Chem.* **2008**, *12*, 1588–1612.
(65) Johansson, L.; Johansson, S.; Nikolajeff, F.; Thorslund, S. *Lab Chip* **2009**, *9*, 297–304.
(66) Yang, Z.; Goto, H.; Matsumoto, M.; Maeda, R. *Electrophoresis* **2000**, *21*, 116–119.

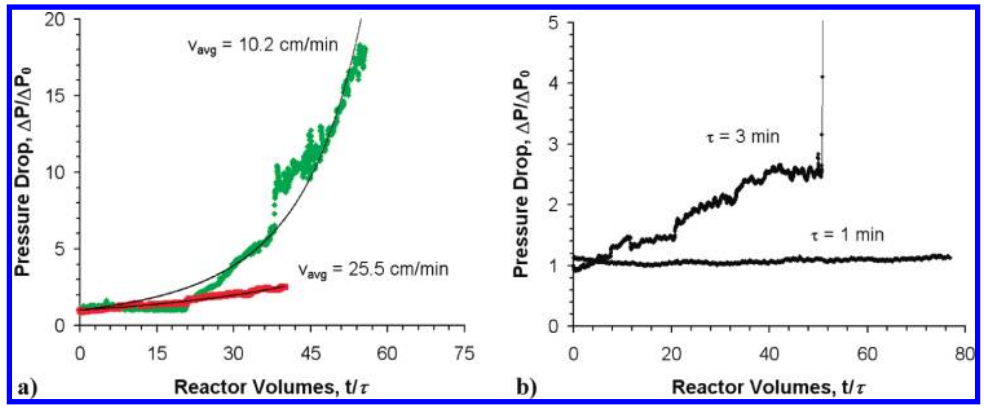

Figure 9. **(a) Influence of changing the average flow velocity from 10.2 to 25.5 cm/min on the dimensionless pressure drop. (b) Reducing the residence time from 3 to 1 min further illustrates that increasing the velocity eliminates significant constriction and bridging.**

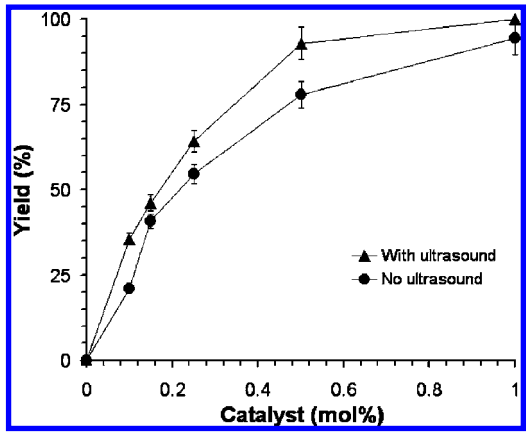

Figure 10. **Influence of ultrasound on product yield for different catalyst loadings.**

Table 1. **Yields for a series of experiments (0.5 mol % Catalyst, $\tau = 1$ min) testing the influence of ultrasound on reaction yield**

exp	yield w/ ultrasound[a]	yield w/o ultrasound[a]
1	86	78
2[b]	80	77
3	86	83
4[b]	85	73
average	84 ± 3	77 ± 3
isolated[c]	80	74

[a] GC yield relative to internal standard. [b] Reaction performed in reverse order. [c] Combined isolated yield for experments 1−4.

was stopped, and the reaction was run for 4 min to reach a new steady state, at which point sample 2 was collected (5 reactor volumes). The injection was stopped, and the reaction was flushed sequentially with dioxane, water, acetone, and dioxane to remove all reagents, salt byproducts, water, and acetone, respectively. The system was then ready for the next experiment. This process was repeated a total of four times, with the second and fourth experiments being performed with sample 1 being the reaction with no sonication and sample 2 being the reaction during sonication. The 8 samples were analyzed by GC and were subsequently combined and isolated (see Table 1). These results support that the acoustic irradiation may have enhanced temperature, mixing, or both. Given that temperature gradients are less significant in microscale systems, one might expect an even more pronounced influence in larger-scale systems. Unstable gas bubbles, smaller than the channel cross-section, were observed in the presence of ultrasound, which may be cavitations that enhance mixing. Further evidence supporting these observations can be seen in Figure S5 and a video (see Supporting Information).

The preparation of 4-methoxy-*N*-phenylaniline represented a case study for understanding how to handle salt byproducts in microsystems during Pd-catalyzed reactions. Figure 11 summarizes a decision roadmap for understanding solids handling while completing the reaction of Scheme 1 and under the conditions presented in this study. As shown, a simple algorithm can be followed to identify the mechanism of microreactor plugging. The choice of reactor design can further be elucidated depending upon the established mechanism. It is important to note that microscale tubular reactors have been the focus of this investigation. Other flow reactor designs, such as continuous stirred tank reactors (CSTR's), have been applied to successfully handle solids.[67] We would not expect clogging in any continuous-flow reactor design when aspect ratios meet the criteria outlined and constriction is managed. In CSTR's, however, transfer tubing inlets and outlets may present the potential for bridging and constriction similar to our findings, which could be addressed via the guidelines described in Figure 11.

On the basis of the data reported in Figure 9b and the residence times investigated, approximately 2.6 g/h of product could be synthesized, whereas synthesis in microflow under these conditions was previously not possible. Just as importantly, the working principles could be extended to other Pd-catalyzed C−N bond formation reactions. Consequently, the laboratory-scale production of fine chemicals prepared with these reactions is possible. Furthermore, microchemical systems may be applied to and the optimization of reaction conditions for individual reactions and complex synthetic pathways. Finally, the ability to handle salt byproducts in microsystems offers the opportunity to use these systems to discover the reaction kinetics and mechanisms of important transformations.

4. Concluding Remarks

We have found that both bridging and constriction take place during Pd-catalyzed amination reactions in microreactors,

(67) Braden, T. M.; Gonzalez, M. A.; Jines, A. R.; Johnson, M. D.; Sun, W. Eli Lilly and Co.: US, 2009.

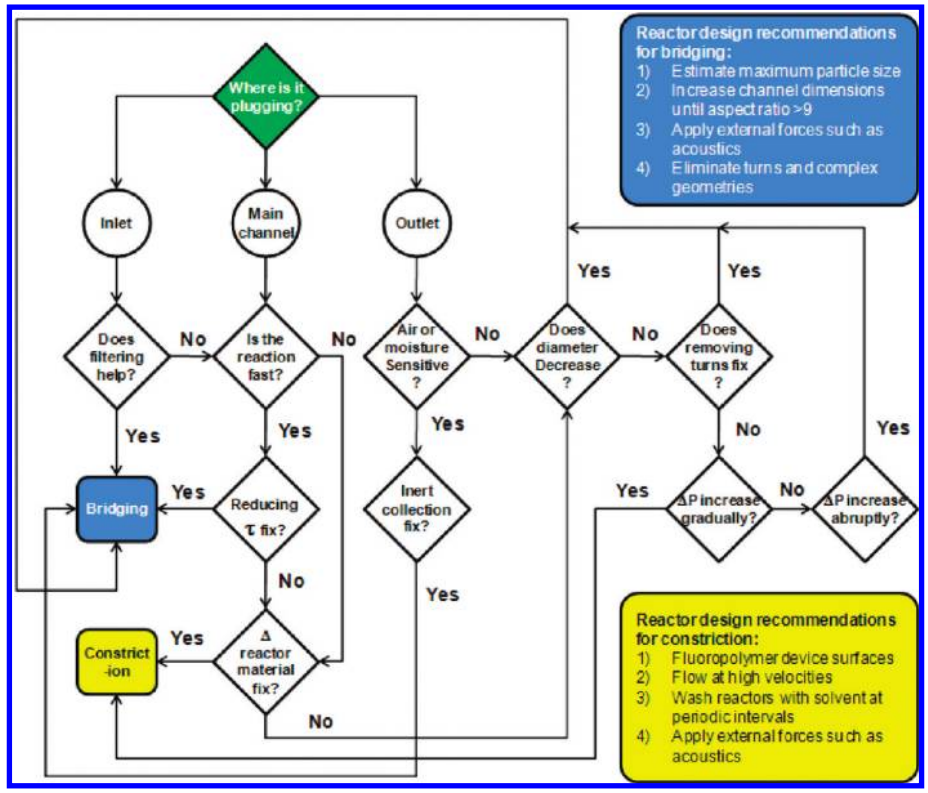

Figure 11. **Decision algorithm for reactor design and solids handling of the reaction in Scheme 1.**

leading to severe plugging. The use of acoustic irradiation reduced the maximum effective particle size of the salt byproduct and thus prevented bridging in PFA capillary-based reactors. It is likely that the magnitude of the acoustic forces exceeded the hydrodynamic and particle-to-particle attractive forces that led to bridging. Slurries of particles, the largest of which had aspect ratios of 28, flowed without severe plugging when acoustic irradiation was applied. In a system that did not include ultrasound, plugging was observed and the aspect ratio of the largest particles was estimated to be 8.9. Constriction was observed to be quite severe in silicon nitride coated devices, and switching to a fluoropolymer capillary did not eliminate the problem. A composite of NaCl and product was formed on the surfaces that were not submerged in the ultrasonic bath and exposed to acoustic irradiation. When the flow rate was increased, the pressure increased at a slower rate. Fitting this data to a constriction model showed a correlation between the rate of wall deposition and flow rate and suggested that a further increase of the flow rate could potentially eliminate clogging due to constriction. Moreover, the presence of acoustic irradiation appeared to enhance the reaction rate, which may be the result of a temperature increase based on the energy emitted from cavitation and/or a result of enhanced mixing. Based on the results reported herein, general guidelines can be prescribed to handle salt byproducts during reactions in microsystems. It is important to limit the particle sizes to aspect ratios of ~9 either by removing them from the reactor before they grow to that size or by imposing an external force such as acoustic irradiation. The filtration of solvents and reagent mixtures can also be important in eliminating potential bridging. Additionally, increasing the flow velocity can help to mitigate constriction. Otherwise, an estimation of the constriction rate can be useful in determining how often solvents need be injected to remove deposits.

Although the handling of solids in microsystems offers new opportunities for chemical reactions that were previously difficult or not attainable, moving forward is not without challenges. Many of the routes to APIs involve solids, which can participate as reactants, products, and catalysts, in addition to salt byproducts. Strategies for handling other types of solids will prove useful for developing efficient flow-based syntheses. Furthermore, the need to operate in both the micro- and macroscale reactors warrants a deeper understanding of solids handling. Additionally, deposition and growth on peripheral equipment, reactors, instruments, and transfer tubing surfaces is an important consideration that needs to be addressed when flowing salts are suspended in organic solvents. Strategies and techniques to remove such deposits will find utility on all scales.

5. Experimental Details

5.1. Microreactor Integration and Control. Standard machining techniques were employed to produce a compression chuck (316 Stainless Steel) with standard #10-32 coned-bottom fluidic ports for each microreactor. The microreactor inlets and outlet were compressed in this chuck (see Figure 1b) using Kalrez o-rings for chemical compatibility, and the chuck was cooled (to 20 °C) using a Thermo Scientific NESLAB RTE-7 refrigerating bath. A Kapton flexible heater (KHLV series, 28 V) and an Omega CN9000 series PID controller were used to control the temperature in the heated section of the microchannel. All fluidic connections were made using $^1/_4$ in.-28 PTFE fittings and PFA tubing ($^1/_{16}$ in. o.d., 500 μm i.d., IDEX Corp.). The pressure transducer was excited using a 10 V power supply,

and the output was recorded using a National Instruments USB 9219 data acquisition card. Images were captured with a high-speed color CCD camera (JAI CV-S3200 series). In the case of capillary PFA reactors, the tubing was submerged in a VWR ultrasonic bath (Model 50HT) filled with deionized water. The bath temperature was monitored via a thermocouple and maintained with a Waage immersion heater controlled by a J-KEM Scientific Gemini PID controller.

5.2. Reagents and Analytical Data. All experiments were carried out using reagent grade solvents, and all solutions were prepared under argon atmospheres. XPhos and the XPhos precatalyst were prepared according to literature procedures.[50,68] Reaction solutions were prepared in screw-cap, oven-dried volumetric flasks. For the clogging experiments, two solutions were prepared. The first solution contained the base (NaO*t*-Bu) and was prepared in 1,4-dioxane. The second solution contained the aryl chloride (4-chloroanisole), amine (aniline), internal standard (biphenyl), and catalyst (XPhos precatalyst) and was also prepared in 1,4-dioxane. Reagents that were solids (biphenyl, XPhos precatalyst, and NaO*t*-Bu) were added to the volumetric flasks that were then evacuated and refilled with argon. This process was repeated a total of 3 times. Liquid reagents were added by syringe, and the solutions were made up to the desired volume with 1,4-dioxane. The base solution was then taken up into a syringe and filtered through a PTFE membrane filter (0.4 μm porosity) into a second flask that had previously been oven-dried and purged with argon. The two solutions were then loaded into syringes and fitted in the syringe pumps for the experiments.

All compounds were characterized by ^{1}H NMR, ^{13}C NMR, IR spectroscopy, and elemental analysis. Copies of the ^{1}H and ^{13}C spectra can be found at the end of the Supporting Information. All ^{13}C NMR spectra were obtained with 1H decoupling. All GC analyses were performed on a Agilent 6890 gas chromatograph with an FID detector using a J & W DB-1 column (10 m, 0.1 mm i.d.).

Analysis of particle sizes exiting the reactors was made possible with a Malvern Mastersizer 2000 laser diffractometer fitted with a Hydro 2000 μP cell. In all cases, samples were collected under argon and diluted by a volumetric factor of 2 with 1,4-dioxane. The analysis was performed by injecting samples ranging from 0.2 to 0.8 mL into the 14.4 mL reservoir of the diffractometer cell that was filled with 1,4-dioxane.

5.2. Workup and Yields. Samples that were collected under argon were diluted with equal volumes of ethyl acetate and water and mixed vigorously. The organic phase was separated, filtered through a short plug of silica gel, and analyzed by GC. Yield and conversion were determined on the basis of the peak area, relative to the internal standard. In two examples, the water phase was extracted with ethyl acetate a total of three times and the organic phases were combined and concentrated. The crude material was then purified by column chromatography (Biotage Isolera, 25 g SNAP column, hexanes and 0−20% ethyl acetate). Isolated yields were found to be in excellent agreement with the GC yields. See the Supporting Information for reaction details.

Acknowledgment

This work has been funded by the Novartis-MIT Center for Continuous Manufacturing.

Supporting Information Available

Discussion of the acoustic waveform with related figures. Discussion of the X-ray diffraction and GCMS analysis of the wall deposit with related figures. Discussion of the influence of acoustics on the reaction by particle analysis and a related figure. Discussion of the general procedure for Pd-catalyzed amination reactions with related NMR spectra. Video showing the gradual clogging of the microreactor. This material is available free of charge via the Internet at http://pubs.acs.org.

Received for review June 2, 2010.

OP100154D

(68) Biscoe, M. R.; Fors, B. P.; Buchwald, S. L. *J. Am. Chem. Soc.* **2008**, *130*, 6686–6687.